Superconductivity-driven negative interfacial magnetization in $YBa_2Cu_3O_{7-\delta}/SrTiO_3/La_{0.67}Sr_{0.33}MnO_3$ heterostructures

Surendra Singh, Harsh Bhatt, Yogesh Kumar, C. L. Prajapat, B. Satpati, C. J. Kinane, S. Langridge, G. Ravikumar and S. Basu

Published version information

Citation: S Singh et al. 'Superconductivity-driven negative interfacial magnetization in $YBa_2Cu_3O_{7-\delta}/SrTiO_3/La_{0.67}Sr_{0.33}MnO_3$ heterostructures. Applied Physics Letters, vol. 116, no. 2 (2020): 022406.

DOI: 10.1063/1.5135578

Applied Physics Letters

Superconductivity-driven negative interfacial magnetization in $YBa_2Cu_3O_{7-\delta}/SrTiO_3/La_{0.67}Sr_{0.33}MnO_3$ heterostructures

Cite as: Appl. Phys. Lett. **116**, 022406 (2020); https://doi.org/10.1063/1.5135578
Submitted: 07 November 2019 . Accepted: 31 December 2019 . Published Online: 13 January 2020

Surendra Singh, Harsh Bhatt, Yogesh Kumar, C. L. Prajapat, B. Satpati, C. J. Kinane, S. Langridge, G. Ravikumar, and S. Basu

Applied Physics Letters ARTICLE scitation.org/journal/apl

Superconductivity-driven negative interfacial magnetization in $YBa_2Cu_3O_{7-\delta}/SrTiO_3/La_{0.67}Sr_{0.33}MnO_3$ heterostructures

Cite as: Appl. Phys. Lett. **116**, 022406 (2020); doi: 10.1063/1.5135578
Submitted: 7 November 2019 · Accepted: 31 December 2019 ·
Published Online: 13 January 2020

Surendra Singh,[1,2,a)] Harsh Bhatt,[1,2] Yogesh Kumar,[1] C. L. Prajapat,[2,3] B. Satpati,[4] C. J. Kinane,[5] S. Langridge,[5] G. Ravikumar,[2,6] and S. Basu[1,2]

AFFILIATIONS

[1]Solid State Physics Division, Bhabha Atomic Research Centre, Mumbai 400085, India
[2]Homi Bhabha National Institute, Anushaktinagar, Mumbai 400094, India
[3]Technical Physics Division, Bhabha Atomic Research Centre, Mumbai 400085, India
[4]Surface Physics and Material Science Division, Saha Institute of Nuclear Physics, 1/AF, Bidhannagar, Kolkata 700064, India
[5]ISIS-Neutron and Muon Source, Rutherford Appleton Laboratory, Didcot, Oxon OX11 0QX, United Kingdom
[6]Scientific Information Resource Division, Bhabha Atomic Research Centre, Mumbai 400085, India

[a)]surendra@barc.gov.in

ABSTRACT

Using spin-polarized neutron reflectivity experiments, we demonstrate an unusual proximity behavior when a superconductor (SC) and a ferromagnet (FM) are coupled through an insulator (I) in $YBa_2Cu_3O_{7-\delta}$ (SC)/$SrTiO_3$ (I)/$La_{0.67}Sr_{0.33}MnO_3$ (FM) heterostructures. We have observed an unexpected magnetic reversal confined to the interface region of the FM below the superconducting transition temperature. The magnetization of the interfacial FM layer at the I/FM interface was found to be aligned opposite to the magnetization of the rest of the FM layer. This result indicates that the Cooper pairs tunnel across the insulator, interact with the local magnetization in the interfacial region (extending ~30 Å) of the FM, and then modify the magnetization at the interface. This unexpected magnetic behavior cannot be explained on the basis of the existing theoretical models. However, the length scale associated here clearly suggests the long-range proximity effect as a result of tunneling of Cooper pairs. The magnetic exchange field-effect across SC/I/FM interfaces driven by tunneling may serve as the basis for application in superconducting spintronic devices.

The proximity effect in superconductor (SC)/ferromagnet (FM) hybrid oxide systems has attracted considerable interest as a result of the fascinating basic physics and also for the possibility to exploit such phenomena in promising applications in superconducting spintronics.[1–6] Earlier studies on SC/FM hybrid systems have combined superconductivity and magnetism and have mainly focused on the injection of spin-polarized quasiparticles into the SC. Subsequently, the tunneling/injection of spin-polarized quasiparticles from an FM to a SC through an insulator (I) in SC/I/FM hybrid oxide heterostructures has been explored with a view to combine spintronics and superconductivity into the so-called superspintronics.[7–9] However, understanding the phenomenon of superconducting carriers tunneling into the FM and its effect on the magnetic state of the FM layer in SC/I/FM oxide heterostructures has remained largely elusive. It is well understood that, for s-wave and d-wave superconductors in SC/FM systems, the spin-singlet Cooper pairs (S = 0) have a limited coherence length even for a weak FM,[1] owing to the magnetic exchange interaction. On the other hand, the Josephson coupling between SCs separated by a thick FM layer clearly suggests the possibility of superconducting order penetrating even into strong FMs.[10–12] The long-range superconducting order at the FM/SC interface was attributed to the presence of spin-triplet Cooper pairs (S = 1) at the interfaces, which are not as sensitive to the exchange field and largely depend on the existence of magnetic inhomogeneities, such as ferromagnetic domain walls or noncollinear magnetization at the interfaces.[2–4]

The most studied SC/FM oxide interfaces are $YBa_2Cu_3O_{7-\delta}$ (YBCO), a d-wave SC, and half-metallic manganites, like $La_{0.67}Ca_{0.33}MnO_3$ (LCMO) or $La_{0.67}Sr_{0.33}MnO_3$ (LSMO), as the FM. Several intriguing interfacial phenomena have been reported for these SC/FM heterostructures.[13–17] However, there are mixed reports

TABLE I. Designed heterostructures with their magnetic and superconducting order temperatures.

Sample	Designed structure	Magnetic transition temperature, T_c	Superconducting transition temperature, T_{sc}
SL	MgO/STO/LSMO	~290 K	…
YSL25	MgO/YBCO/STO(25Å)/LSMO		~65 K
YSL50	MgO/YBCO/STO(50Å)/LSMO		
YL	MgO/YBCO/LSMO		

regarding the appearance of spin-triplet Cooper pairs in the YBCO/LCMO (or LSMO) systems.[18–20] Recently, Visani *et al.*[21] demonstrated the possibility of long-range proximity effects between YBCO and LCMO due to the interference effects between a quasiparticle and electrons in the conductance spectra across the YBCO/LCMO interface and the correlation length was found to be as high as the thickness of the LCMO layer.

The key factor that has been established behind the observed long-range propagation of superconducting correlations into a half metal-based FM/SC system is a conversion from spin-singlet to spin-triplet pairing near the interfaces.[22,23] Introducing an insulator layer between the FM and SC is expected to hinder the propagation of long-range superconducting correlations into the FM unless there is tunneling of Cooper pairs through the insulator. Using polarized neutron reflectivity (PNR), we recently found strong magnetic modulation below the superconducting transition temperature (T_{sc}) in YBCO/$SrTiO_3$ (STO)/LCMO hybrid heterostructures grown on STO substrates.[24] While PNR results clearly indicated a magnetic modification at the interface caused by superconductivity, there was uncertainty involved because of the closeness of the magnetic transition temperature ($T_c \sim 150$ K) of LCMO with the structural phase transition temperature of STO[25,26] in this system. Paull *et al.*[27] also confirmed the magnetic modulation in the YBCO/STO/LCMO heterostructure below T_{sc}.

Here, we report an unusual magnetization at the interface of an LSMO layer through an insulator (STO) in YBCO/STO/LSMO heterostructures, using the depth-sensitive PNR technique,[24,27–31] below T_{sc}. We observed the emergence of a negative magnetization (magnetization opposite to the applied field) in the LSMO layer over a thickness of $\sim 30 \pm 5$ Å, at the STO/LSMO interface in the YBCO/STO/LSMO heterostructure below T_{sc}. The PNR results revealed that suppression of the magnetization at the STO/LSMO interface above T_{sc} is an intrinsic phenomenon. However, the negative magnetization at the STO/LSMO interface below T_{sc} in YBCO/STO/LSMO heterostructures is solely dependent on superconductivity.

We grew a number of hybrid heterostructures by pulsed laser deposition on single-crystal MgO (001) substrates (supplementary material). Four heterostructures (Table I) discussed here are henceforth known as YSL25, YSL50, YL, and SL, where letters Y, S, and L stand for YBCO, STO, and LSMO, respectively. Two (three) letters in a sample code indicate a bilayer (trilayer). The numbers 25 and 50 in the trilayer codes are the nominal thicknesses (in angstrom) of the STO layer. Thus, YSL25 identifies a heterostructure with a layer structure: MgO/YBCO/STO(25 Å)/LSMO.

The x-ray diffraction (XRD) scans on the log scale for YSL25, YSL50, YL, and SL heterostructures are shown in Fig. 1. A comparison of XRD data from the heterostructures suggests ordered and strongly textured growth along (00*l*) directions, similar to the heterostructures grown on STO substrates.[24,32] The YBCO (002) diffraction peak shown in the inset (i) of Fig. 1 clearly shows the interference fringes (indicated by the vertical arrow) around the diffraction peak and suggests the high quality of interfaces. The microstructure of an identically grown YBCO/STO/LSMO heterostructure is visible in the cross-sectional high-resolution transmission electron microscopy (TEM) image shown in the inset (ii) of Fig. 1. A combination of XRD, TEM, and selected area electron diffraction together with a depth-dependent elemental concentration profile of each element further confirms the formation of highly ordered heterostructures (Figs. S1 and S2 in the supplementary material). The layer structure and macroscopic magnetic properties of these heterostructures have been characterized using x-ray reflectivity (XRR)[28–31] and a superconducting quantum interface device (SQUID) magnetometer, respectively (Fig. S3 in the supplementary material). The XRR results are given in Table S3 (supplementary material). We obtained a Curie temperature (T_c) ≈ 290 K and a $T_{sc} \approx 65$ K for these heterostructures, which are consistent with previous results for LSMO films[29,33–35] and YBCO films.[16,24,36]

To obtain the depth profile of magnetization in heterostructures across T_{sc}, we have used the PNR technique, because of its depth sensitivity for ordered magnetism.[28–31] PNR experiments were performed on a POLREF reflectometer at the ISIS neutron and muon source, UK. The PNR data were taken in an applied in-plane magnetic field (H) of 500 Oe at different temperatures after cooling the heterostructures in the same field. A schematic of the PNR geometry is shown in the inset of Fig. 2(a). The spin-dependent R^+ and R^- reflectivities, where the superscript plus (minus) sign indicates the neutrons with spin parallel

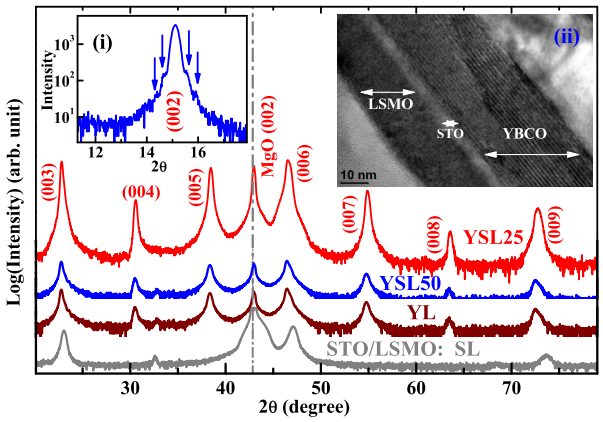

FIG. 1. (a) XRD data on a log scale (y-axis) for heterostructures grown on MgO. Inset (i) shows (002) reflection of YBCO. Inset (ii) shows the cross-sectional TEM image of a similarly grown YBCO/STO/LSMO heterostructure.

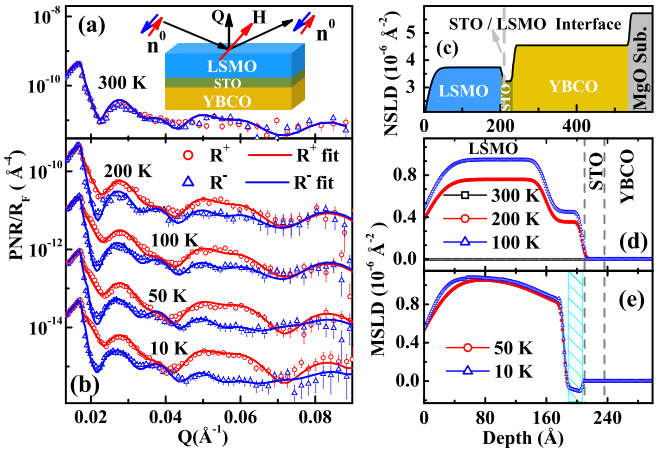

FIG. 2. (a) PNR data for the YSL25 at 300 K. The inset of (a) shows the schematic of the PNR experiment. (b) PNR data for YSL25 at different temperatures, which are vertically shifted for better visualization. (c) NSLD depth profiles extracted from PNR data. (d) and (e) MSLD depth profiles of YSL25 at different temperatures extracted from PNR data.

(antiparallel) to the direction of H, are measured as a function of the wave vector transfer, Q ($=\frac{4\pi \mathrm{Sin}(\theta)}{\lambda}$, with θ and λ being the angle of incidence and wavelength of the neutron). Reflectivity data presented here are represented as reflectivity normalized to the asymptotic value of the Fresnel reflectivity, R_F ($= 16\pi^2/Q^4$).[28–31] The depth profiles of the nuclear and magnetic scattering length densities (NSLD and MSLD) obtained from the PNR correspond to the depth profile of the chemical and in-plane magnetization, respectively.[28–31]

Figure 2(a) shows the PNR data for YSL25 at 300 K. The difference between R^+ and R^- reflectivities contains information on the magnetic depth profile.[28–31] PNR data at 300 K indicate no ferromagnetism, as the difference $R^+ - R^- \sim 0.0$, which is consistent with the SQUID measurements. The NSLD depth profile at 300 K is shown in Fig. 2(c), and the structural parameters obtained from PNR are also given in Table S3 (supplementary material). PNR data (open circles and triangles) and the corresponding fits (solid lines) for YSL25 at different temperatures across T_{sc} are depicted in Fig. 2(b). The MSLD depth profiles obtained from the PNR data at low temperatures are plotted in Figs. 2(c) and 2(d), as a function of the depth from the surface.

PNR data for YSL25 above T_{sc} (100 and 200 K) show a suppression of the magnetization in the LSMO layer up to ∼50 Å from the STO/LSMO interface, with MSLD values of 4.4×10^{-7} Å^{-2} (at 100 K) and 3.5×10^{-7} Å^{-2} (at 200 K). There are various reports suggesting both a reduction and enhancement in the magnetization of the LSMO near a STO/LSMO interface, which are attributed to strain, oxygen content, deposition conditions, and charge discontinuity.[33–35] In view of this, we have considered several magnetization models to fit the PNR data for YSL25 at 100 K, which are shown in Figs. S4(a)–S4(c) (supplementary material). Different magnetic models comprising enhanced, suppressed, and zero (depleted) interfacial magnetization at the STO/LSMO interface [Figs. S4(d)–S4(f) in the supplementary material] are statistically compared for the quality of each fit. We observe that the model of a reduced magnetization for the LSMO layer (thickness ∼50 Å) at the STO/LSMO interface best describes the PNR data above T_{sc} (100 and 200 K). The magnetization of the interfacial LSMO layer increases upon decreasing the temperature from 200 to 100 K. Remarkably, we obtained an unusual negative MSLD of $\sim -1.0 \times 10^{-7}$ Å^{-2} ($\sim -36 \pm 20$ emu/cc) for a region of the LSMO layer of thickness $\sim 30 \pm 5$ Å at the STO/LSMO interface below T_{sc} (50 and 10 K) [shaded region in Fig. 2(e)]. A comparison of fits of the PNR data at 10 K, assuming zero magnetization (depleted), reduced (positive), and negative magnetization, for the interfacial LSMO layer is shown in Fig. S5 (supplementary material), suggesting that a layer with small negative magnetization at the interface better fits the PNR data at 10 K. The magnetization in rest of the LSMO layer was $\sim 380 \pm 25$ emu/cc (MSLD $\sim 9.1 \times 10^{-7}$ Å^{-2}), which is in agreement with earlier measurements for the 40 nm LSMO film[37] but lower than its bulk value (∼550 emu/cc).[35] The unexpected magnetic behavior across T_{sc} cannot be explained on the basis of the existing theoretical models. However, experimental findings reported here clearly suggest a long-range proximity effect in this FM/I/SC system with tunneling geometry, which modifies magnetization near the interface in the heterostructure below T_{sc}.

Any tunneling effect should strongly depend on the thickness of the insulating barrier. In order to see the effect of the insulating (STO) layer thickness on the magnetization depth profile in the YBCO/STO/LSMO heterostructures across T_{sc}, we also studied another trilayer YSL50, with a thicker (∼50 Å) STO layer. Figure 3(a) shows the PNR data from YSL50 at different temperatures. Figures 3(b) and 3(c) show the NSLD and MSLD depth profiles obtained from PNR data. Like YSL25, we obtained a reduced magnetization at the STO/LSMO interface above T_{sc} (∼100 K) and a negative magnetization below

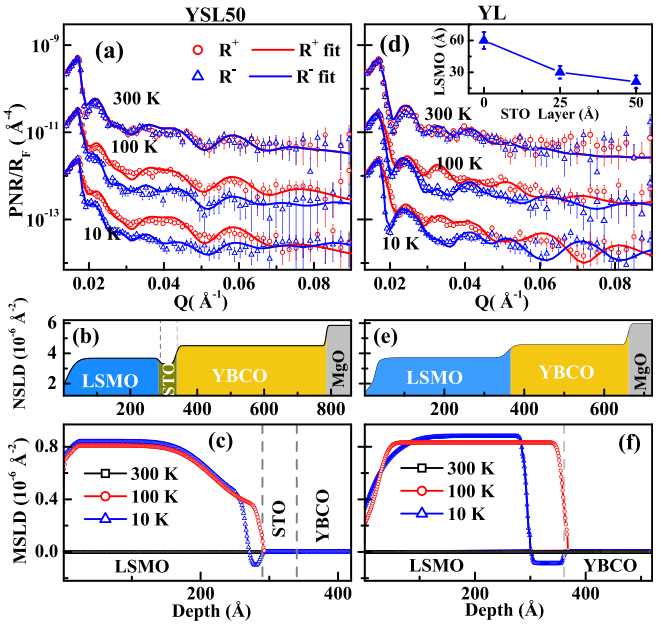

FIG. 3. (a) PNR data at a different temperature for YSL50. NSLD (b) and MSLD (c) depth profiles of YSL50. (d) PNR data at different temperatures from YL. NSLD (e) and MSLD (f) depth profiles of YL. Reflectivities at different temperatures are vertically shifted for better visualization. The inset of (d) shows the variation of the interfacial LSMO layer (showing negative magnetization) thickness with the STO layer thickness in heterostructures.

T_{sc} (50 and 10 K). The thickness of the LSMO layer at the STO/LSMO interface, which shows negative magnetization, has reduced to ~20 ± 5 Å, whereas the magnetization at the interface remains the same (~−36 emu/cc), as obtained for YSL25. The length scales (STO thickness and interfacial LSMO layer) associated with these two systems, YSL25 and YSL50, imply that the SC correlation may involve a flow of Cooper pairs and are thus a direct consequence of having a long-range proximity effect through tunneling. The idea of tunneling of Cooper pairs has been proposed theoretically, and modulation in interfacial magnetic properties was expected due to such tunneling.[38,39] The TEM and reflectivity measurements from YBCO/STO/LSMO systems clearly suggested a uniform layer of STO sandwiched between the YBCO and LSMO layers. This indicates that there are no pinholes across the YBCO-LSMO layers, which can give rise to the transfer of Cooper pairs from YBCO to LSMO through STO.

We have also probed the proximity effect at the YBCO/LSMO interface (FM is in direct contact with SC) in a YBCO/LSMO bilayer (heterostructure YL) across T_{sc}. PNR measurements for YL [Fig. 3(d)], under similar conditions as adopted for YSL25 and YSL50, were also carried out at different temperatures across T_{sc}. The NSLD and MSLD profiles of the YL obtained from PNR data are shown in Figs. 3(e) and 3(f). There are two distinctive features we observed in the YL with respect to the trilayers. First, we observed a uniform magnetization [Fig. 3(f)] for the whole LSMO layer above T_{sc} (100 K), unlike in case YSL25 and YSL50, where we obtained suppressed magnetization at the STO/LSMO interface, and second, we obtained a negative magnetization (~−35 emu/cc) for the LSMO layer over a much larger thickness (~60 ± 7 Å) at the YBCO/LSMO interface [Fig. 3(f)] below T_{sc} (10 K). Magnetic modification over a larger length scale of ~60 Å below T_{sc} in the YL further indicates the possibility of injection of Cooper pairs at the interface and their long-range propagation in the FM. A variation in the thickness of the interfacial LSMO layer with negative magnetization as a function of STO layer thickness in these heterostructures is shown in the inset of Fig. 3(d), suggesting a reduction in the interfacial LSMO layer thickness with the increase in the thickness of the insulator (STO) layer between FM and SC layers.

Having observed the suppression in the magnetization of the interfacial LSMO layer at the STO/LSMO interface in YSL25 and YSL50, above T_{sc}, the temperature-dependent magnetization depth profile at the STO/LSMO interface "without an SC layer" is another important issue we addressed here. We studied a bilayer of STO/LSMO (heterostructure SL). Figure 4(a) shows the PNR data from SL at different temperatures. Figure 4(b) shows the NSLD depth profile of the SL obtained from PNR data at 300 K. Figures 4(c)–4(e) show the MSLD depth profiles at different temperatures. Temperature-dependent PNR data clearly suggest that a suppressed magnetization in an interfacial LSMO layer of thickness ~48 ± 6 Å, best describes the measurements. Different magnetization models at interfaces were also considered for fitting the PNR data at 100 and 10 K and are given in Fig. S6 (supplementary material). A comparison of the fits for different models clearly suggested that the model with reduced interfacial magnetization best describes the PNR data ≤200 K.

It is noted that the magnetization reduction at the STO/LSMO interface in SL ≤ 200 K is due to the intrinsic property of the LSMO/STO interface and not just due to the structural phase transition of STO near 110 K.[25,26] To correlate the reduced magnetization at the STO/LSMO interface with strain, we estimated the strain for the

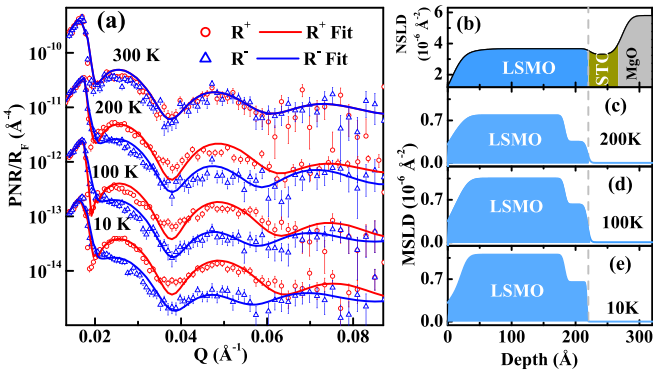

FIG. 4. (a) PNR data for SL at different temperatures, which are vertically shifted for better visualization. (b) NSLD depth profile of the SL heterostructure. (c)–(e) MSLD depth profile extracted from the PNR data at different temperatures.

LSMO layers in different heterostructures using XRD data (Table S2 in the supplementary material), which did not show any correlation of strain with reduced magnetization. The reduction in magnetization for the interfacial LSMO layer in the STO/LSMO layer was also observed earlier and was attributed to different other effects, e.g., oxygen deficiency,[33] doping conditions,[40] orbital reconstruction,[41] and a change in orbital ordering.[42] PNR data from SL also suggested that the magnetization of the LSMO/STO interface increases upon decreasing the temperature, which is an expected trend for any ferromagnetic layer. In contrast, the magnetization at the LSMO/STO interface in YSL (YSL25 and YSL50) heterostructures showed negative (reduced) magnetization below (above) T_{sc}, suggesting superconductivity dependent phenomena.

Since the magnetic field applied during PNR measurements was small (~500 Oe), the contribution of it to the magnetization depth profile, assuming (i) the YBCO layer is in the Abrikosov mixed state[43] and (ii) Meissner response (~0.07 emu/cc) of a thin superconducting film,[24,43] was very small, which is below the detection limit of PNR. In addition, the Abrikosov mixed state is mostly observed for thick (greater than few hundred nanometers) YBCO films and contributes negligibly for induced magnetization in YBCO films due to an in-plane applied field of ~500 Oe.[44] Thus, these effects will not influence the magnetization depth profile obtained from PNR for these heterostructures.

Negative magnetization in the SC layer in the SC-FM-SC system was earlier ascribed to the inverse proximity effect.[2] The inverse proximity effect for nonoxide systems has been observed over a much longer length scale into the SC layer.[45,46] Recently, Mironov *et al.*[46] proposed a theory of long-range electromagnetic proximity effect suggesting a strong spread of the magnetic field into the SC from the FM. Our results show the direct proximity effect for the YBCO/LSMO system and through tunneling in YBCO/STO/LSMO systems. However, we observed a negative magnetization for the interfacial LSMO layer. We believe that Cooper pair, tunnel through the insulating STO layer from YBCO to LSMO in the YBCO/STO/LSMO system and interact with the local magnetization (phase separation at different length scales) in the LSMO layer, which may give rise to negative spin accumulation (spin randomness) contributing to small negative magnetization (depletion) at the interface in YBCO/STO/LSMO

heterostructures, whereas larger penetration was observed in the YBCO/LSMO system. The existence of spontaneous spin accumulation has also been reported in a Josephson junction between a spin-singlet and a spin-triplet superconductor[47] as well as in an SC/FM/SC Josephson junction with strong spin–orbit coupling in the FM layer.[48]

In summary, we have experimentally observed negative magnetization for an interfacial LSMO layer in the YBCO/STO/LSMO trilayers (tunneling geometry) and in the YBCO/LSMO bilayer (proximity geometry) below T_{sc}. PNR data provided direct evidence that the YBCO/STO/LSMO and the YBCO/LSMO heterostructures exhibit a SC driven negative magnetization for the interfacial LSMO layer (thickness ∼30–60 Å) at the STO/LSMO and the YBCO/LSMO interfaces, respectively. The thickness of the interfacial LSMO layer decreases upon increasing the thickness of the insulator (STO) layer, suggesting that the tunneling of Cooper pairs is a possible mechanism for magnetization modulation below T_{sc}. The length scale associated with this tunneling-driven proximity effect strongly suggests the presence of long-range Cooper pairs in this system. However, future theoretical analysis is necessary to elucidate if such tunneling of Cooper pairs is possible in such strongly textured oxide heterostructures. Magnetization modulation in an SC/I/FM system driven by tunneling may serve as a basis for envisaging device applications in superconducting spintronics.

See the supplementary material for XRD from individual FM, I, and SC films and XRR measurements from heterostructures. Squid measurements from FM/I/SC and a comparison of magnetization modeling at different temperatures for FM/SC and FM/I/SC systems are also provided.

Y.K. acknowledges the support from the Department of Science and Technology (DST), India, via the DST INSPIRE faculty research grant (No. DST/INSPIRE/04/2015/002938). We thank the ISIS Neutron and Muon source for the provision of beam time.

REFERENCES

[1]A. I. Buzdin, Rev. Mod. Phys. **77**, 935–976 (2005).
[2]F. S. Bergeret, A. F. Volko, and K. B. Efetov, Rev. Mod. Phys. **77**, 1321–1373 (2005).
[3]J. Linder and J. W. A. Robinson, Nat. Phys. **11**, 307–315 (2015).
[4]F. S. Bergeret, A. F. Volkov, and K. B. Efetov, Phys. Rev. Lett. **86**, 4096–4099 (2001).
[5]A. K. Feofanov, V. A. Oboznov, V. V. Bolginov, J. Lisenfeld, S. Poletto, V. V. Ryazanov, A. N. Rossolenko, M. Khabipov, D. Balashov, A. B. Zorin, P. N. Dmitriev, V. P. Koshelets, and A. V. Ustinov, Nat. Phys. **6**, 593–597 (2010).
[6]Z. Yang, M. Lange, A. Volodin, R. Szymczak, and V. Moshchalkov, Nat. Mater. **3**, 793–798 (2004).
[7]C.-C. Fu, Z. Huang, and N.-C. Yeh, Phys. Rev. B **65**, 224516 (2002).
[8]T. Nojima, M. Iwata, T. Hyodo, S. Nakamura, and N. Kobayashi, Physica C **412–414**, 147–151 (2004).
[9]L. Fratila, I. Maurin, and C. Dubourdieu, Appl. Phys. Lett. **86**, 122505 (2005).
[10]J. W. A. Robinson, J. D. S. Witt, and M. G. Blamire, Science **329**, 59–61 (2010).
[11]K. Senapati, M. G. Blamire, and Z. H. Barber, Nat. Mater. **10**, 849–852 (2011).
[12]M. Eschrig, Phys. Today **64**(1), 43–49 (2011).
[13]V. Peña, C. Visani, J. Garcia-Barriocanal, D. Arias, Z. Sefrioui, C. Leon, J. Santamaria, and C. A. Almasan, Phys. Rev. B **73**, 104513 (2006).
[14]T. Holden, H.-U. Habermeier, G. Cristiani, A. Golnik, A. Boris, A. Pimenov, J. Humlíček, O. I. Lebedev, G. Van Tendeloo, B. Keimer, and C. Bernhard, Phys. Rev. B **69**, 064505 (2004).
[15]J. Chakhalian, J. W. Freeland, H.-U. Habermeier, G. Cristiani, G. Khaliullin, M. van Veenendaal, and B. Keimer, Science **318**, 1114 (2007).
[16]J. Hoppler, J. Stahn, C. Niedermayer, V. K. Malik, H. Bouyanfif, A. J. Drew, M. Rössle, A. Buzdin, G. Cristiani, H.-U. Habermeier, B. Keimer, and C. Bernhard, Nat. Mater. **8**, 315 (2009).
[17]G. Yashwant, C. L. Prajapat, G. Ravikumar, S. Soltan, G. Christiani, and H.-U. Habermeier, J. Magn. Magn. Mater. **324**, 1406–1409 (2012).
[18]K. Dybko, K. Werner-Malento, P. Aleshkevych, M. Wojcik, M. Sawicki, and P. Przyslupski, Phys. Rev. B **80**, 144504 (2009).
[19]I. Fridman, L. Gunawan, G. A. Botton, and J. Y. T. Wei, Phys. Rev. B **84**, 104522 (2011).
[20]Y. Kalcheim, T. Kirzhner, G. Koren, and O. Millo, Phys. Rev. B **83**, 064510 (2011).
[21]C. Visani, Z. Sefrioui, J. Tornos, C. Leon, J. Briatica, M. Bibes, A. Barthelemy, J. Santamaria, and J. E. Villegas, Nat. Phys. **8**, 539–543 (2012).
[22]M. Eschrig and T. Lofwander, Nat. Phys. **4**, 138 (2008).
[23]J. Linder, M. Cuoco, and A. Sudbø, Phys. Rev. B **81**, 174526 (2010).
[24]C. L. Prajapat, S. Singh, A. Paul, D. Bhattacharya, M. R. Singh, S. Mattauch, G. Ravikumar, and S. Basu, Nanoscale **8**, 10188 (2016).
[25]R. Blinc, B. Zalar, V. V. Laguta, and M. Itoh, Phys. Rev. Lett. **94**, 147601 (2005).
[26]S. Singh, T.-Y. Chien, J. R. Guest, and M. R. Fitzsimmons, Phys. Rev. B **85**, 115450 (2012).
[27]O. H. C. Paull, A. V. Pan, G. L. Causer, S. A. Fedoseev, A. Jones, X. Liu, A. Rosenfeld, and F. Klose, Nanoscale **10**, 18995 (2018).
[28]S. Singh, M. R. Fitzsimmons, T. Lookman, J. D. Thompson, H. Jeen, A. Biswas, M. A. Roldan, and M. Varela, Phys. Rev. Lett. **108**, 077207 (2012).
[29]S. Singh, J. T. Haraldsen, J. Xiong, E. M. Choi, P. Lu, D. Yi, X.-D. Wen, J. Liu, H. Wang, Z. Bi, P. Yu, M. R. Fitzsimmons, J. L. MacManus-Driscoll, R. Ramesh, A. V. Balatsky, J.-X. Zhu, and Q. X. Jia, Phys. Rev. Lett. **113**, 047204 (2014).
[30]M. R. Fitzsimmons and C. Majkrzak, *Modern Techniques for Characterizing Magnetic Materials* (Springer, New York, 2005), Chap. 3, pp. 107–155.
[31]S. Singh, M. Swain, and S. Basu, Prog. Mater. Sci. **96**, 1–50 (2018).
[32]C. L. Prajapat, S. Singh, D. Bhattacharya, G. Ravikumar, S. Basu, S. Mattauch, J.-G. Zheng, T. Aoki, and A. Paul, Sci. Rep. **8**, 3732 (2018).
[33]D. Schumacher, A. Steffen, J. Voigt, J. Schubert, T. Bruckel, H. Ambaye, and V. Lauter, Phys. Rev. B **88**, 144427 (2013).
[34]M. Huijben, Y. Liu, H. Boschker, V. Lauter, R. Egoavil, J. Verbeeck, S. G. E. te Velthuis, G. Rijnders, and G. Koster, Adv. Mater. Interfaces **2**, 1400416 (2015).
[35]E.-J. Guo, T. Charlton, H. Ambaye, R. D. Desautels, H. N. Lee, and M. R. Fitzsimmons, ACS Appl. Mater. Interfaces **9**, 19307 (2017).
[36]C. B. Eom, J. Z. Sun, B. M. Lairson, S. K. Streiffer, A. F. Marshall, K. Yamamoto, S. M. Anlage, J. C. Bravman, T. H. Geballe, S. S. Laderman, R. C. Taber, and R. D. Jacowitz, Physica C **171**, 354 (1990).
[37]A. J. Grutter, D. A. Gilbert, U. S. Alaan, E. Arenholz, B. B. Maranville, J. A. Borchers, Y. Suzuki, K. Liu, and B. J. Kirby, Appl. Phys. Lett. **108**, 082405 (2016).
[38]T. Zhou, Phys. Rev. Lett. **106**, 167001 (2011).
[39]T. Zhou, Y. Gao, and Z. D. Wang, Phys. Rev. B **99**, 104517 (2019).
[40]J. J. Kavich, M. P. Warusawithana, J. W. Freeland, P. Ryan, X. Zhai, R. H. Kodama, and J. N. Eckstein, Phys. Rev. B **76**, 014410 (2007).
[41]M. Huijben, L. W. Martin, Y.-H. Chu, M. B. Holcomb, P. Yu, G. Rijnders, D. H. A. Blank, and R. Ramesh, Phys. Rev. B **78**, 094413 (2008).
[42]A. Tebano, C. Aruta, S. Sanna, P. G. Medaglia, G. Balestrino, A. A. Sidorenko, R. De Renzi, G. Ghiringhelli, L. Braicovich, V. Bisogni, and N. B. Brookes, Phys. Rev. Lett. **100**, 137401 (2008).
[43]Y. Khaydukov, R. Morari, L. Mustafa, J.-H. Kim, T. Keller, S. Belevski, A. Csik, L. Tagirov, G. Logvenov, A. Sidorenko, and B. Keimer, J. Supercond. Novel Magn. **28**, 1143 (2015).
[44]L. F. Cohen and H. J. Jensen, Rep. Prog. Phys. **60**, 1581 (1997).
[45]R. I. Salikhov, I. A. Garifullin, N. N. Garif'yanov, L. R. Tagirov, K. Theis-Bröhl, K. Westerholt, and H. Zabel, Phys. Rev. Lett. **102**, 087003 (2009).
[46]S. Mironov, A. S. Melnikov, and A. Buzdin, Appl. Phys. Lett. **113**, 022601 (2018).
[47]K. Sengupta and V. M. Yakovenko, Phys. Rev. Lett. **101**, 187003 (2008).
[48]M. Alidoust and K. Halterman, New J. Phys. **17**, 033001 (2015).